Title

Identification of NK Cell Subpopulations That Differentiate HIV-Infected Subject Cohorts with Diverse Levels of Virus Control.

Journal

Journal of Virology, 93(7)

ISSN

0022-538X

Authors

Pohlmeyer, Christopher W
Gonzalez, Veronica D
Irrinki, Alivelu
et al.

Publication Date

2019-04-01

DOI

10.1128/jvi.01790-18

Peer reviewed

AMERICAN SOCIETY FOR MICROBIOLOGY | Journal of Virology®

PATHOGENESIS AND IMMUNITY

Identification of NK Cell Subpopulations That Differentiate HIV-Infected Subject Cohorts with Diverse Levels of Virus Control

Christopher W. Pohlmeyer,[a] Veronica D. Gonzalez,[b] Alivelu Irrinki,[a] Ricardo N. Ramirez,[a] Li Li,[a] Andrew Mulato,[a] Jeffrey P. Murry,[a] Aaron Arvey,[a]* Rebecca Hoh,[c] Steven G. Deeks,[c] George Kukolj,[a]* Tomas Cihlar,[a] Stefan Pflanz,[a]* Garry P. Nolan,[b] Gundula Min-Oo[a]

[a]Gilead Sciences, Inc., Foster City, California, USA
[b]Department of Microbiology and Immunology, Baxter Laboratory in Stem Cell Biology, Stanford University, Stanford, California, USA
[c]Division of HIV, Infectious Diseases and Global Medicine, University of California, San Francisco, San Francisco, California, USA

ABSTRACT HIV infection is controlled immunologically in a small subset of infected individuals without antiretroviral therapy (ART), though the mechanism of control is unclear. $CD8^+$ T cells are a critical component of HIV control in many immunological controllers. NK cells are also believed to have a role in controlling HIV infection, though their role is less well characterized. We used mass cytometry to simultaneously measure the levels of expression of 24 surface markers on peripheral NK cells from HIV-infected subjects with various degrees of HIV natural control; we then used machine learning to identify NK cell subpopulations that differentiate HIV controllers from noncontrollers. Using CITRUS (cluster identification, characterization, and regression), we identified 3 NK cell subpopulations that differentiated subjects with chronic HIV viremia (viremic noncontrollers [VNC]) from individuals with undetectable HIV viremia without ART (elite controllers [EC]). In a parallel approach, we identified 11 NK cell subpopulations that differentiated HIV-infected subject groups using k-means clustering after dimensionality reduction by t-neighbor stochastic neighbor embedding (tSNE) or linear discriminant analysis (LDA). Among these additional 11 subpopulations, the frequencies of 5 correlated with HIV DNA levels; importantly, significance was retained in 2 subpopulations in analyses that included only cohorts without detectable viremia. By comparing the surface marker expression patterns of all identified subpopulations, we revealed that the $CD11b^+$ $CD57^-$ $CD161^+$ Siglec-7^+ subpopulation of $CD56^{dim}$ $CD16^+$ NK cells are more abundant in EC and HIV-negative controls than in VNC and that the frequency of these cells correlated with HIV DNA levels. We hypothesize that this population may have a role in immunological control of HIV infection.

IMPORTANCE HIV infection results in the establishment of a stable reservoir of latently infected cells; ART is usually required to keep viral replication under control and disease progression at bay, though a small subset of HIV-infected subjects can control HIV infection without ART through immunological mechanisms. In this study, we sought to identify subpopulations of NK cells that may be involved in the natural immunological control of HIV infection. We used mass cytometry to measure surface marker expression on peripheral NK cells. Using two distinct semisupervised machine learning approaches, we identified a $CD11b^+$ $CD57^-$ $CD161^+$ Siglec-7^+ subpopulation of $CD56^{dim}$ $CD16^+$ NK cells that differentiates HIV controllers from noncontrollers. These cells can be sorted out for future functional studies to assess their potential role in the immunological control of HIV infection.

KEYWORDS elite controller, machine learning, mass cytometry, human immunodeficiency virus, natural killer cells

Citation Pohlmeyer CW, Gonzalez VD, Irrinki A, Ramirez RN, Li L, Mulato A, Murry JP, Arvey A, Hoh R, Deeks SG, Kukolj G, Cihlar T, Pflanz S, Nolan GP, Min-Oo G. 2019. Identification of NK cell subpopulations that differentiate HIV-infected subject cohorts with diverse levels of virus control. J Virol 93:e01790-18. https://doi.org/10.1128/JVI.01790-18.

Editor Frank Kirchhoff, Ulm University Medical Center

Address correspondence to Gundula Min-Oo, gundula.min-oo@gilead.com.

* Present address: Aaron Arvey, Department of Microbiology and Immunology, University of California, San Francisco, San Francisco, California, USA; George Kukolj, Exploratory Science Center, Merck, Cambridge, Massachusetts, USA; Stefan Pflanz, Cancer Immunology and Immune Modulation, Boehringer Ingelheim, Biberach, Germany.

Received 9 October 2018
Accepted 19 January 2019
Accepted manuscript posted online 30 January 2019
Published 21 March 2019

HIV is a retrovirus that establishes a life-long latent infection and remains a global health burden despite highly effective therapies. HIV-infected individuals treated with suppressive antiretroviral therapy maintain undetectable HIV plasma viral loads, but this treatment is not curative due to the slow decay of a reservoir of latently infected cells (1, 2). Interruption of antiretroviral therapy is typically followed by a robust rebound of viremia; thus, therapy must be continued for the life of the individual. Intriguingly, a subset of HIV-infected individuals can control HIV load in the absence of antiretroviral therapy (3–6). Viremic controllers (VC) maintain a low HIV load (40 to 2,000 copies of HIV RNA/ml of plasma), and elite controllers (EC) maintain an undetectable HIV load ($\leq$40 copies of HIV RNA/ml of plasma). The mechanism of immunological control in these subjects is not fully understood.

NK cells and cytotoxic T lymphocytes (CTLs) have both been implicated in immunological control of HIV infection (7). Certain major histocompatibility complex class I (MHC-I) molecules are overrepresented in controller cohorts, most notably, HLA-B*57 and HLA-B*27 (8, 9), and several studies have demonstrated a quantitatively and qualitatively superior CTL response in EC and VC who possess these protective MHC alleles (10–15). Nevertheless, a substantial proportion of controllers lack protective MHC alleles and may control HIV infection through a non-CTL mechanism (16). NK cells may contribute to the controller phenotype, both in the absence of (17) and in conjunction with (18–20) protective MHC-I alleles. Recently, in a case of early immunological control of HIV by a subject lacking protective MHC-I alleles, researchers found an effective cytotoxic NK effect without robust CTL activity (21).

In peripheral blood, classical NK cells are historically identified as $CD56^{bright}$ $CD16^{-}$ (cytokine-producing) and $CD56^{dim}$ $CD16^{+}$ (cytotoxic) (22). A nonclassical NK cell population ($CD56^{-}$ $CD16^{+}$ $CD7^{+}$) with reduced functional capacity is expanded in HIV-infected subjects and may comprise recently activated cells that have become anergic (23–27). This subset has been described in other chronic viral infections, such as hepatitis C virus (HCV), but is largely absent in HIV-negative (HN) donors (28, 29).

NK cell activity is regulated by a balance of signals downstream of multiple activating and inhibitory receptors (30), including the killer cell immunoglobulin-like receptor (KIR), C-type lectin receptor (e.g., CD94), and natural cytotoxic receptor (NCR) families. These receptors interact with MHC-I, adhesion molecules, and costimulatory molecules, among others.

Interactions between HLA-B Bw4-80Ile alleles (including HLA-B*57) and KIR3DL1 as well as homozygosity for KIR3DS1 have been shown to be protective against HIV acquisition (31, 32) and progression (18–20), and viral evolution to escape pressure applied by KIR molecules has been described previously (33). A recent study demonstrated the importance of immunological control of HIV by NK cells that express NKG2A (34). In addition, upon activation with alpha interferon (IFN-α), NK cells are able to kill HIV-infected $CD4^{+}$ T cells via activating NKG2D and NKp46 receptors (35), though the HIV Nef protein has been shown to be able to downregulate ligands for both NKG2D and KIRs (36, 37). Additionally, NCR molecules are downregulated during chronic HIV infection, possibly contributing to the dysfunction of NK cells (38).

Prior studies have characterized NK cells from HIV controllers (39) or compared NK cell functionality to clinical parameters (40). In this study, we used mass cytometry to simultaneously profile 24 NK cell surface markers on the single-cell level in 93 subjects with differing degrees of HIV infection control, including both VC and EC. We used semisupervised machine learning approaches to identify and quantify NK cell subpopulations associated with the ability to control HIV infection.

RESULTS

Subject characterization. Subjects were categorized into 5 groups based on HIV load and antiretroviral therapy status (see Materials and Methods). Clinical characteristics of the participating subjects are presented in Table S1 in the supplemental material. The distributions of subject $CD4^{+}$ T cell counts and viral loads are shown in Fig. 1A.

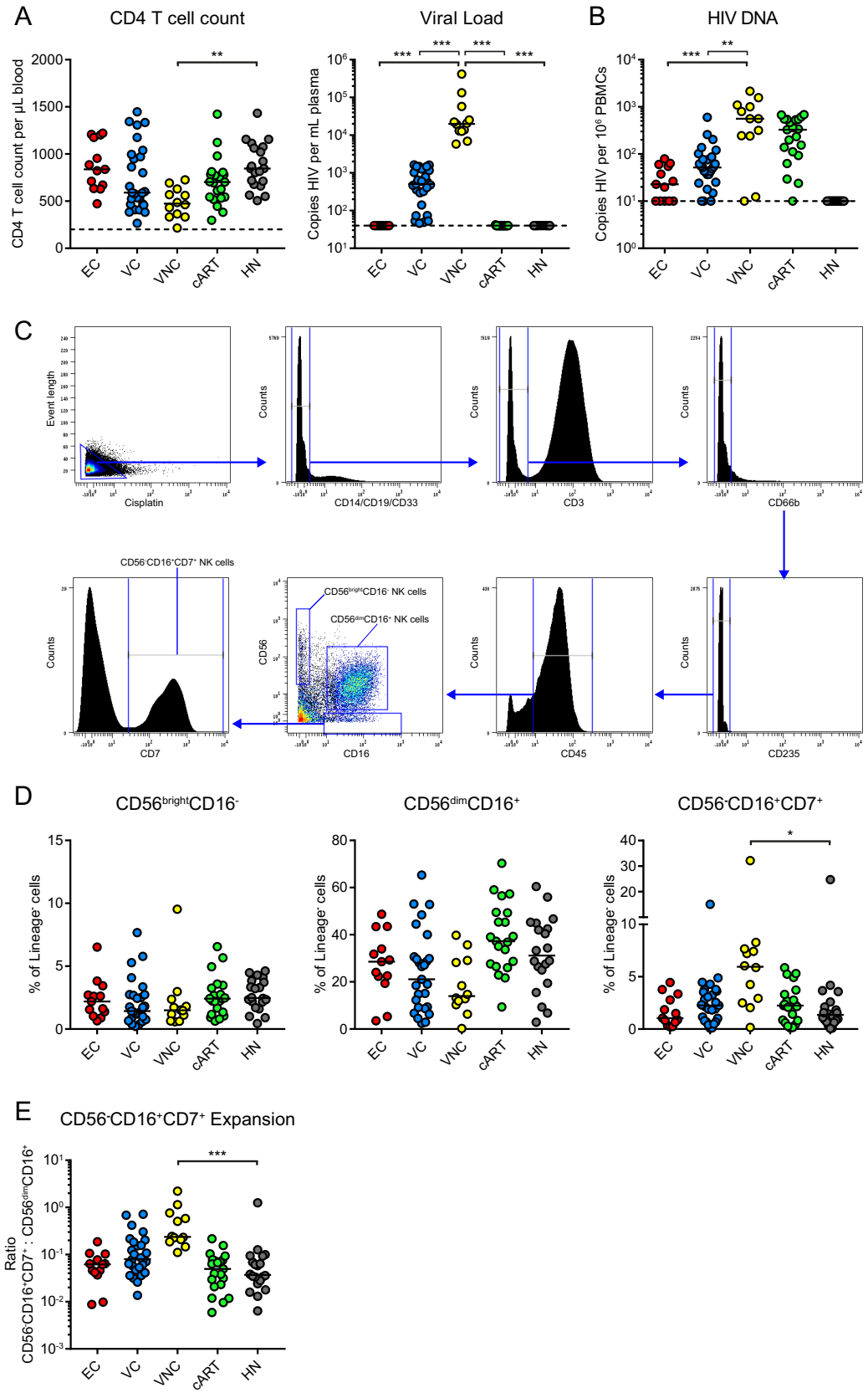

FIG 1 Study subject characterization. A total of 93 subjects were recruited for participation in this study (EC, $n = 13$, red; VC, $n = 27$, blue; VNC, $n = 12$, yellow; cART, $n = 21$, green; HN, $n = 20$, gray). (A) Subject peripheral blood $CD4^+$ T cell count (left) and HIV load (right). All subjects had a $CD4^+$ T cell count above 200 cells/μl of blood (left, dotted line). The limit of

(Continued on next page)

We estimated HIV reservoir size for HIV-infected subjects with a previously published PCR-based approach (41, 42). Although PCR-based total HIV DNA measurements in peripheral blood mononuclear cells (PBMCs) detect defective provirus and unintegrated DNA and may not accurately measure reservoir size (43, 44), these measurements can distinguish groups of HIV-infected subjects and can be used as a proxy for reservoir size. Our data are consistent with other reports of HIV DNA reservoir measurements in the subject groups representing combination antiretroviral therapy (cART) and viremic noncontrollers (VNC) (41) (Fig. 1B). HIV DNA levels were higher in most VNC subjects than in cART subjects, likely due to detection of actively infected cells, though this difference was not statistically significant. VC and EC subjects had significantly lower HIV DNA levels than VNC subjects ($P = 0.0051$ and $P = 0.0001$, respectively).

Mass cytometry NK cell phenotyping. To fully explore the repertoire of NK cell subsets by simultaneously interrogating the expression levels of a wide variety of activating and inhibitory receptors, we utilized a comprehensive mass cytometry approach. We designed and qualified an NK cell-focused panel (Table S2) of 38 antibodies (Abs). A total of 34 antibodies passed our quality control, as 4 antibodies had either minimal staining or high background levels. All 10 antibodies chosen for cell lineage identification passed quality control. All 93 subjects were subjected to immune phenotyping by mass cytometry in 6 independent runs. Run-to-run variability was minimal, as determined by t-neighbor stochastic neighbor embedding (tSNE) (data not shown). We interrogated mass cytometry results in two ways: first, we measured correlations between individual surface marker expression frequencies and the size of the HIV DNA reservoir; second, we used semisupervised machine learning approaches to identify NK cell subpopulations that differed in abundance among the enrolled HIV-infected subject groups.

Expansion of CD56$^-$ NK cells occurs in viremic subjects. Because NK cell subset imbalance has been observed in subjects chronically infected with HIV (23–27), we measured the frequencies of the two major NK cell subsets (CD56^{bright} CD16$^-$ and CD56^{dim} CD16$^+$) and of the more recently described CD56$^-$ CD16$^+$ CD7$^+$subset in all HIV-infected subject groups (23) to verify that the NK cell subset distribution in our subject cohort reflected previous findings (23–27). The gating strategy used is shown in Fig. 1C. There were no significant differences in the frequencies of either of the two major NK cell subsets across HIV-infected subject groups, compared to HN, after adjusting for multiple comparisons (Fig. 1D). We observed a higher frequency of CD56$^-$ CD16$^+$ CD7$^+$ NK cells within lineage-negative cells (CD3$^-$ CD14$^-$ CD19$^-$ CD33$^-$ CD45$^+$ CD66b$^-$ CD235$^-$) in VNC than in HN ($P = 0.014$, false discovery rate [FDR] adjusted). Additionally, we saw a significantly higher ratio of CD56$^-$ CD16$^+$ CD7$^+$ cells to CD56^{dim} CD16$^+$ cells in VNC than in HN ($P < 0.0005$, FDR adjusted), suggesting that CD56$^-$ CD16$^+$ CD7$^+$ cells may have expanded in VNC subjects (Fig. 1E).

Frequencies of individual markers on NK cell subsets correlate with HIV DNA. To identify the NK cell subpopulations whose frequencies correlated with immunological control, we calculated correlations between the frequencies of NK cell subsets expressing individual markers and viral load, CD4$^+$ T cell count, or HIV DNA levels. We observed a number of individual NK cell markers that correlated with viral load or CD4$^+$ T cell count, some of which have been previously reported as differentially expressed in HIV controllers, including LIR1 (45), though none of these correlations withstood

FIG 1 Legend (Continued)
detection for viral load was 40 copies of HIV RNA/ml of plasma (right, dotted line). (B) HIV DNA measurement for each subject. The limit of quantitation was 10 copies/10^6 PBMCs (dotted line). (C) Events were first gated on intact cells, followed by dead cell discrimination gating. NK cells were identified as CD3$^-$ CD14$^-$ CD19$^-$ CD33$^-$ CD45$^+$ CD66b$^-$ CD235$^-$ and then differentiated by CD56, CD16, and CD7 expression. (D) Frequency of NK cell subsets within lineage-negative (CD3$^-$ CD14$^-$ CD19$^-$ CD33$^-$ CD45$^+$ CD66b$^-$ CD235$^-$) PBMCs. (E) Expansion of CD56$^-$ CD16$^+$ CD7$^+$ NK cells as measured by the ratio of CD56$^-$ CD16$^+$ CD7$^+$ to CD56^{dim} CD16$^+$ NK cells. Each color-filled point represents an individual subject, and horizontal lines represent the group medians. Significance was calculated using a Kruskal Wallis test with a *post hoc* Dunn's test. Each subject group was compared to VNC. *P* values were adjusted by multiplying by the number of comparisons made (Bonferroni correction). *, $P < 0.05$; **, $P < 0.005$; ***, $P < 0.0005$.

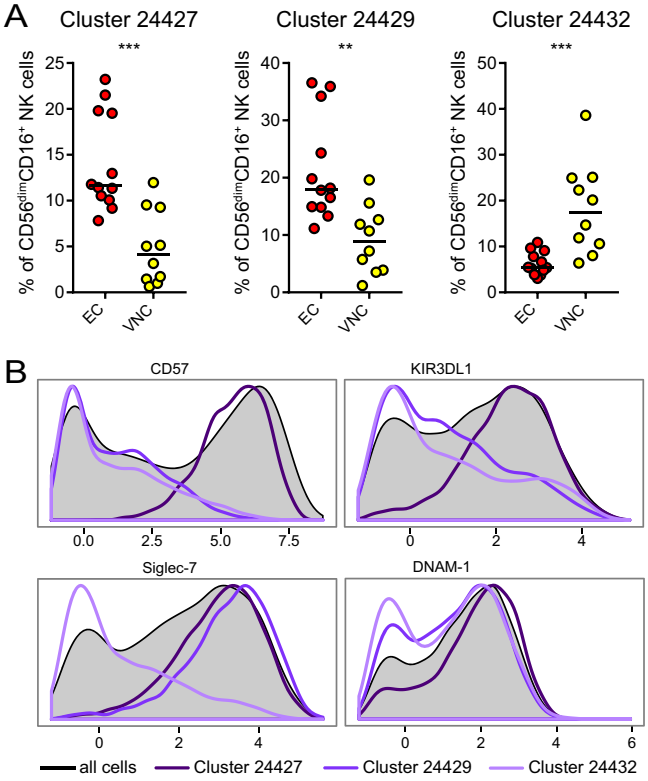

FIG 2 CITRUS analysis of NK cell subsets revealed three clusters within CD56^{dim} CD16^{+} NK cells that differentiate EC from VNC. (A) Frequency of cells within clusters identified by CITRUS to differentiate EC (red) and VNC (yellow) subject groups. Each color-filled point represents an individual subject, and horizontal lines represent the group median. Significance was calculated using the Kruskal Wallis test. *P* values were further adjusted by multiplying by the number of comparisons made (Bonferroni correction). **, $P < 0.005$; ***, $P < 0.0005$. (B) Expression intensity of markers that distinguish bulk CD56^{dim} CD16^{+} NK cells (black line, shaded background) from the cells identified in cluster 24427, 24429, or 24432 (lines of gradating purple color). Histograms representing the expression intensities of all NK markers measured are shown in Fig. S1. *x*-axis data represent marker expression intensity; *y*-axis data represent frequency.

Bonferroni correction for multiple comparisons ($P > 0.05$). The only significant correlations remaining after correction for multiple comparisons were those between HIV DNA and expression of either CD62L or Siglec-7 on CD56^{dim} CD16^{+} NK cells ($P = 0.001$ and $P = 0.001$, respectively) or of either CD27 or Siglec-7 on CD56^{-} CD16^{+} CD7^{+} NK cells ($P = 0.011$ and $P = 0.026$, respectively) (data not shown). These results corroborate findings from multiple previous studies (26, 46–48).

CD56^{dim} CD16^{+} NK cell subpopulations that differentiate EC from VNC. In order to discover novel NK cell subpopulations defined on the basis of multiple markers, we analyzed the entire mass cytometry panel concurrently. We first used CITRUS (49) to identify NK cell subpopulations that differentiated groups of HIV-infected subjects. In order to minimize noise, our analysis included only NK cells and NK cell-related markers (i.e., lineage markers were used to gate NK cells but were excluded from downstream analyses). HIV-infected subject groups were compared in a pairwise fashion. Using CITRUS, we could not distinguish any HIV-infected subject groups from one another using the CD56^{bright} CD16^{-} NK cell subset (≤15% model cross-validation error rate). However, we were able to differentiate EC from VNC using the CD56^{dim} CD16^{+} NK cell subset. Three clusters of cells identified by CITRUS within CD56^{dim} CD16^{+} NK cells (clusters 24427, 24429, and 24432) differentiated EC from VNC (Fig. 2A). The expression levels of selected markers that helped differentiate these clusters of cells are shown in Fig. 2B; the expression levels of all NK markers measured are shown in Fig. S1 in the supplemental material.

Dimensionality reduction followed by k-means clustering revealed NK cell subpopulations that differentiated multiple HIV-infected subject groups. As a distinct approach, we performed supervised and unsupervised dimensionality reduction prior to cluster identification and pairwise comparisons of cluster frequencies. We concatenated cells from subjects across all HIV-infected subject groups and ran principal-component analysis (PCA), linear discriminant analysis (LDA), or tSNE. PCA and tSNE are both unsupervised dimensionality reduction algorithms that preserve the information in a data set while allowing identification of new clusters. In contrast, LDA is a supervised dimensionality reduction algorithm that separates data points using defined response variables as a guide to maximize separation. Using ACCENSE (50), we used the first two dimensions from each dimensionality reduction algorithm for k-means clustering to define NK cell subpopulations. To our knowledge, using a supervised dimensionality reduction algorithm prior to clustering is a novel approach to identify cellular populations that differentiate subject groups from high-parameter mass cytometry data sets.

Dimensionality reduction by PCA performed poorly, as the information contained in the first principal component was explained almost entirely by expression of CD57. From two-dimensional coordinates generated by tSNE, we identified one subpopulation within the $CD56^-$ $CD16^+$ $CD7^+$ NK cells (cluster 1) that differentiated viremic subjects (VC, VNC) from aviremic subjects (EC, cART, HN) (Fig. 3A and B). This NK cell subpopulation expressed higher levels of KIR3DL1 (Fig. 3C), suggesting a loss of this inhibitory marker in response to viremia.

From two-dimensional coordinates generated by LDA, k-means clustering identified five subpopulations within $CD56^{bright}$ $CD16^-$ NK cells (clusters 2 to 6) that differentiated viremic subjects (VC, VNC) from aviremic subjects (EC, cART, HN) (Fig. 3D and E). The relevant markers for identification of these NK cell subpopulations are shown in Fig. 3F. The cells in clusters 2 to 4, which were less abundant in viremic subjects, showed high levels of CD11b and CD161 expression. Cells expressing these markers are matured and play a proinflammatory role (51, 52); CD161-expressing NK cells have been shown previously to be depleted in viremic HIV-infected subjects (52). The cells in clusters 5 to 6, which were more abundant in viremic subjects, had higher expression of DNAM-1 and NKp46, suggesting that they were matured and active NK cells (53, 54).

Also, using LDA followed by k-means clustering, we identified an additional five subpopulations within the $CD56^{dim}$ $CD16^+$ NK cells (clusters 7 to 11) that differentiated VNC from other groups of HIV-infected subjects (Fig. 4A). Similarly to the cells in clusters 2 to 4, the cells in clusters 7 to 11 expressed elevated levels of CD11b and CD161, but they also showed increased expression of Siglec-7 and lacked expression of CD57 (Fig. 4B). Clusters 7 to 11 were differentially abundant between VNC and EC, with intermediate frequencies observed in the VC and cART groups. The cells identified by cluster 10 were also more frequent within the EC group than within the HN group ($P = 0.001$, FDR adjusted).

We next performed a linear regression analysis to determine whether the frequencies of the cells in clusters 1 to 11 were associated with HIV DNA levels. HIV DNA levels correlated significantly with the frequencies of cells identified by clusters 7 to 11 (Fig. 5A); excluding the viremic subjects from the analysis (Fig. 5B), clusters 8 and 10 maintained significant correlations with HIV DNA levels. Importantly, this suggests that these clusters were correlated with integrated HIV DNA as an approximate indicator of the frequency of cells containing proviral DNA and representing the overall infection burden in T cells rather than a latent replication-competent virus reservoir. This conclusion was unaffected by converting the HIV DNA copy number per 10^6 PBMCs to the HIV DNA copy number per 10^6 $CD4^+$ T cells for correlative analysis (data not shown).

The $CD11b^+$ $CD57^-$ $CD161^+$ $Siglec\text{-}7^+$ subpopulation of $CD56^{dim}$ $CD16^+$ NK cells differentiated HIV-infected subject groups. The expression levels of CD11b, CD161, CD57, and Siglec-7 on cells identified by clusters 7 to 11 followed broadly similar distribution patterns (Fig. 4B). When clusters 7 to 11 were combined, we

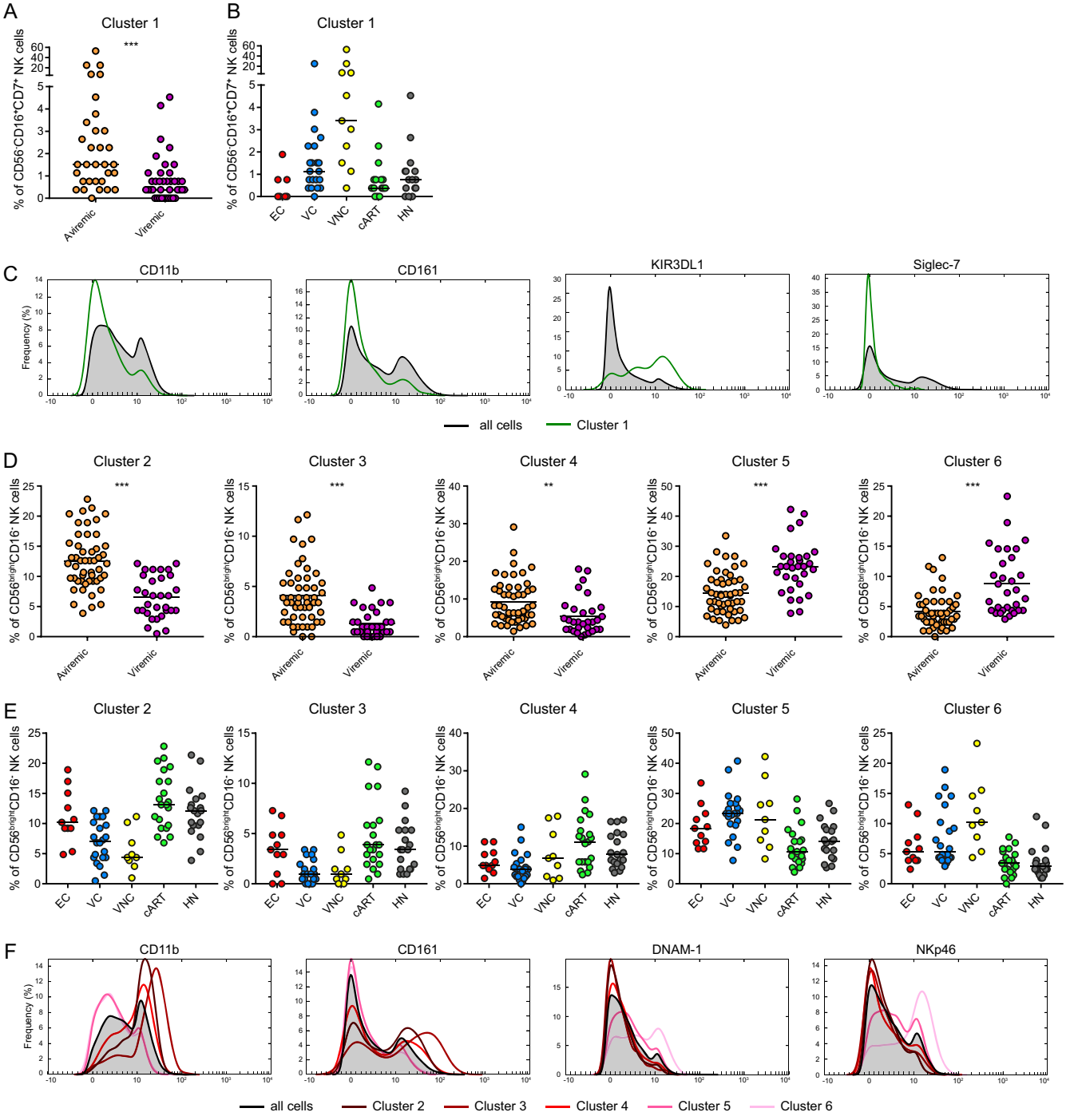

FIG 3 Clusters identified after dimensionality reduction and k-means clustering differentiate viremic subjects from aviremic subjects. (A and B) Frequency of cells within cluster identified after running tSNE analysis on CD56$^-$ CD16$^+$ CD7$^+$ NK cells followed by k-means clustering. Each color-filled point represents an individual subject (orange, EC, cART, HN; purple, VC, VNC), and horizontal lines represent the group median. Significance testing was done by the Kruskal Wallis test with a *post hoc* Dunn's test. ***, $P < 0.0005$. (C) Expression intensity of markers that distinguish bulk CD56$^-$ CD16$^+$ CD7$^+$ NK cells (black line, shaded background) from the cells identified in cluster 1 (green line). Histograms representing the expression intensities of all NK markers measured are shown in Fig. S2. *x*-axis data represent marker expression intensity. (D and E) Frequency of cells within clusters identified after running LDA on CD56^{bright} CD16$^-$ NK cells followed by k-means clustering. Each color-filled point represents an individual subject (orange, EC, cART, HN; purple, VC, VNC), and horizontal lines represent the group median. Significance testing was done by Kruskal Wallis test with a *post hoc* Dunn's test. *P* values were further adjusted by multiplying by the number of comparisons made (Bonferroni correction). **, $P < 0.005$; ***, $P < 0.0005$. (F) Expression intensity of markers that distinguish bulk CD56^{bright} CD16$^-$ NK cells (black line, shaded background) from the cells identified in clusters 2 to 6 (lines in gradations of red). Histograms representing the expression intensities of all NK markers measured are shown in Fig. S3. *x*-axis data represent marker expression intensity.

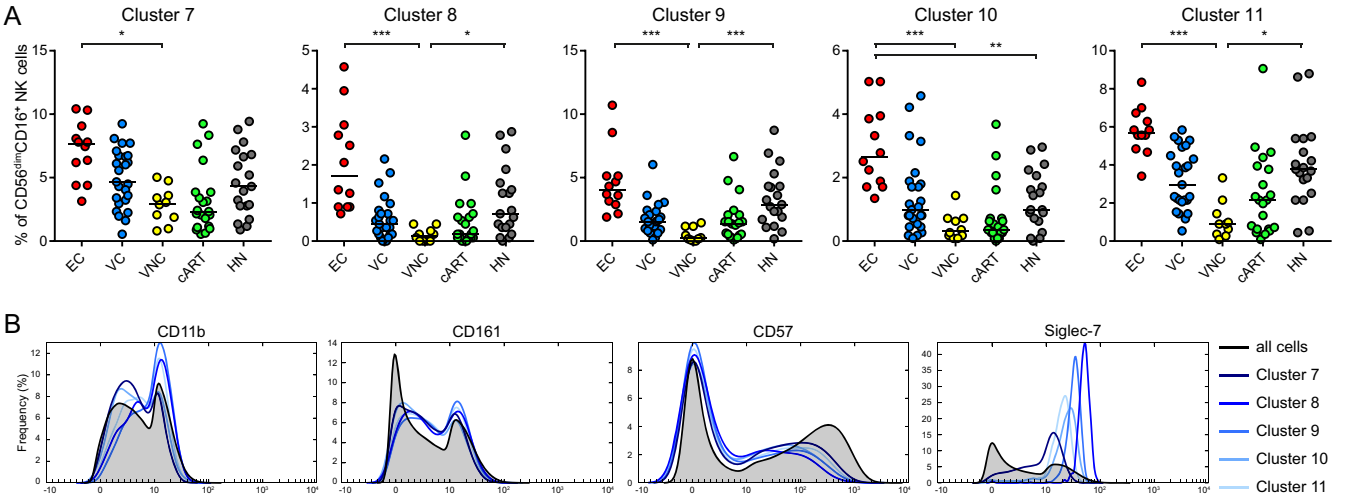

FIG 4 Several clusters identified after dimensionality reduction differentiate subject groups. (A) Frequency of cells within clusters identified after running LDA on CD56^{dim} CD16^{+} NK cells. Each color-filled point represents an individual subject, and horizontal lines represent the group median. Significance was tested using the Kruskal Wallis test with a *post hoc* Dunn's test. Each subject group was compared to VNC. Additionally, EC and HN groups were tested for normal distribution (D'Agostino & Pearson, Shapiro-Wilk, and KS normality tests); cluster frequencies with distributions that did not significantly differ from the normal distribution were compared by unpaired *t* test, and cluster frequencies with distributions that did significantly differ from the normal distribution were compared by Mann-Whitney test. *P* values were all further adjusted by multiplying by the number of comparisons made (Bonferroni correction). *, $P < 0.05$; **, $P < 0.005$; ***, $P < 0.0005$. (B) Expression intensity of markers that distinguish bulk CD56^{dim} CD16^{+} NK cells (black line, shaded background) from the cells identified in clusters 7 to 11 (lines of gradating blue color). Histograms representing the expression intensities of all NK markers measured are shown in Fig. S4. *x*-axis data represent marker expression intensity.

observed that the distribution of these markers on these cells showed a profile similar to that seen with the cells in cluster 24429 identified by CITRUS. These relationships are shown in Fig. 6A. This suggests that two disparate machine learning algorithms independently converged on identification of a similar NK cell subpopulation that showed a high level of expression of CD11b, CD161, and Siglec-7 and a low level of expression of CD57.

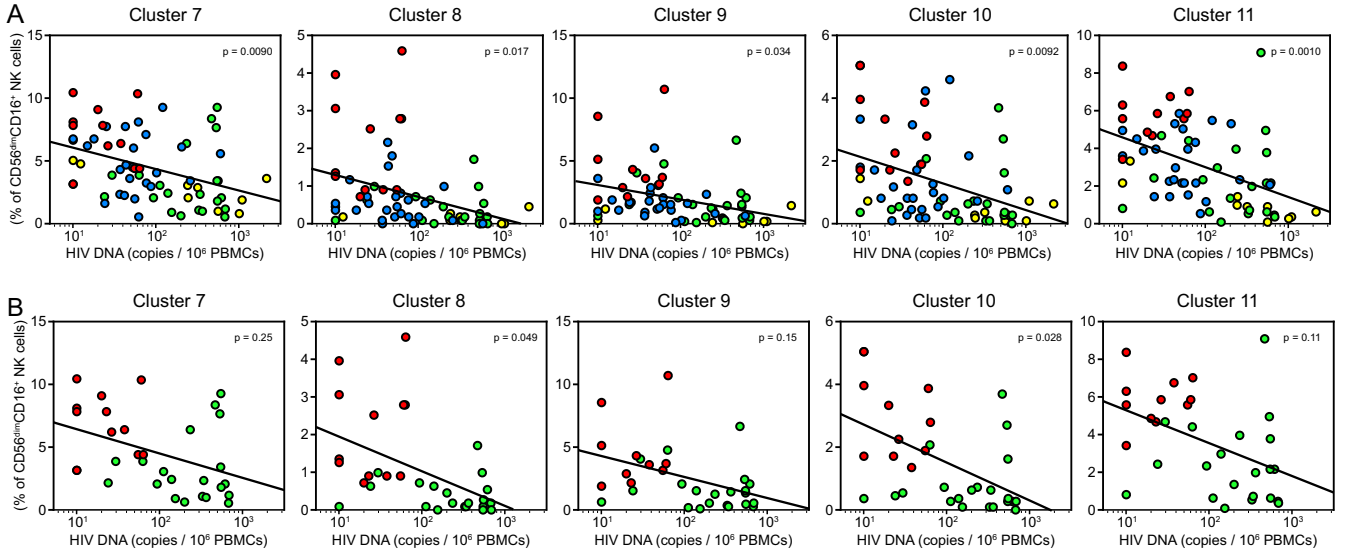

FIG 5 Frequencies of clusters 7 to 11 correlate with HIV DNA levels. The frequency of cells within clusters 1 to 11 was correlated with the log value of HIV DNA measurements using an ordinary least-squares regression. (A) All HIV-infected subject groups were included in the analysis. Only correlations with slopes that differ significantly from 0 are shown. (B) Only aviremic HIV-infected subjects (EC, cART) were included in the analysis. Each color-filled point represents an individual subject, and each solid line represents the line corresponding to the best fit. *P* values were adjusted by multiplying by the number of comparisons made (Bonferroni correction) and are displayed in the upper right corner of each individual graph. EC, red; VC, blue; VNC, yellow; cART, green.

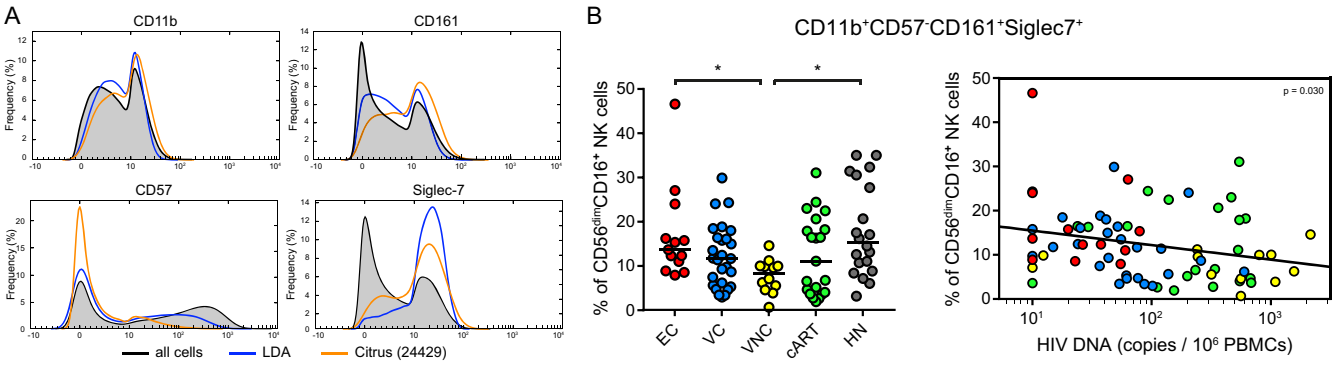

FIG 6 Computational approaches identify a novel NK cell population that differentiates HIV-infected subject groups. (A) Histograms representing the expression intensities of markers that distinguish all CD56^{dim} CD16^{+} NK cells (black line, shaded background) from the cells identified in clusters 7 to 11 combined (LDA, blue line) or in cluster 24429 (CITRUS, gold line). *x*-axis data represent marker expression intensity. (B) Frequency of CD11b^{+} CD57^{-} CD161^{+} Siglec-7^{+} cells within the CD56^{dim} CD16^{+} NK cell subset (left). The frequency of the CD11b^{+} CD57^{-} CD161^{+} Siglec-7^{+} CD56^{dim} CD16^{+} NK cell subpopulation was correlated with the log value of HIV DNA measurements using an ordinary least-squares regression (right). Each color-filled point represents an individual subject, and horizontal lines represent the group median. Significance was calculated using the Kruskal Wallis test with a *post hoc* Dunn's test. Each subject group was compared to VNC. *, $P < 0.05$.

Using manual gating approaches, we compared the frequencies of CD11b^{+} CD57^{-} CD161^{+} Siglec-7^{+} cells within the CD56^{dim} CD16^{+} NK cell population across the HIV-infected subject groups and the HN group (Fig. 6B, left). This subpopulation was more frequently observed in EC and HN than in VNC ($P = 0.048$ and $P = 0.010$, respectively). Though CD161^{+} cells within the CD56^{dim} CD16^{+} NK cell population have been previously shown to differentiate cART and VNC subjects (52), all 4 markers were necessary to identify a subpopulation that differentiated the HIV-infected subject groups in this study. We confirmed the expression of CD57 and CD161 from these mass cytometry findings in an independent experiment performed using traditional flow cytometry to verify that these markers alone were not sufficient to identify the NK cell subpopulation (data not shown). The frequency of this NK cell subpopulation, either per 10^6 PBMCs or per 10^6 CD4^{+} T cells, correlated with HIV DNA measurements (Fig. 6B, right).

Increased functionality in the CD11b^{+} CD57^{-} CD161^{+} Siglec-7^{+} subpopulation of CD56^{dim} CD16^{+} NK cells. In order to determine if the CD11b^{+} CD57^{-} CD161^{+} Siglec-7^{+} subpopulation of CD56^{dim} CD16^{+} NK cells had enhanced functional capacity, we used standard NK cell stimulation conditions to measure the levels of cytokine production and degranulation. Enriched NK cells showed low production of IFN-γ without stimulation. Under conditions of stimulation with interleukin-12 (IL-12)/IL-18, CD11b^{+} CD57^{-} CD161^{+} Siglec-7^{+} cells showed significantly more IFN-γ production than CD11b^{-}, CD161^{-}, or Siglec-7^{-} subpopulations (Fig. 7A). We next cocultured enriched NK cells with K562 cells; K562 cells are MHC class I deficient and act as NK cell targets. NK cells cultured without K562 cells had a low background level of degranulation. We observed a significantly higher frequency of degranulation in the CD11b^{+} CD57^{-} CD161^{+} Siglec-7^{+} subpopulation of CD56^{dim} CD16^{+} NK cells than in CD11b^{-}, CD161^{-}, or Siglec-7^{-} subpopulations (Fig. 7B). The CD57^{+} subpopulation, which is believed to be "antigen-experienced" (55), showed high levels of cytokine production and degranulation; there was no significant difference between CD11b^{+} CD57^{-} CD161^{+} Siglec-7^{+} cells and CD57^{+} cells under either of the sets of stimulation conditions.

DISCUSSION

We used a multifaceted approach to identify novel NK cell phenotypes and subpopulations associated with immunological control of HIV. A key advantage of mass cytometry over traditional flow cytometry is the ability to generate high-parameter data sets to interrogate many cellular phenotypic differences across subject cohorts simultaneously, considering a comprehensive receptor repertoire rather than individual

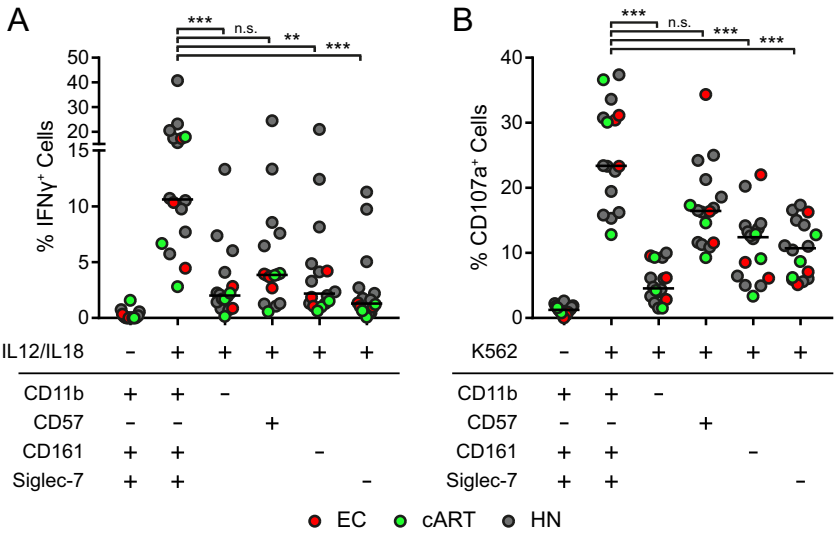

FIG 7 Functional activity of the CD11b$^+$ CD57$^-$ CD161$^+$ Siglec-7$^+$ subpopulation of CD56^{dim} CD16$^+$ NK cell subset. (A) Frequency of IFN-γ producing NK cells with or without stimulation with IL-12/IL-18. + and − above the horizontal line indicate whether stimulation was added; + and − below the horizontal line indicate the expression of indicated marker on gated CD56^{dim} CD16$^+$ NK cell subpopulation. (B) Frequency of degranulating NK cells as measured by CD107a analysis during stimulation with or without coculture of K562 target cells. + and − above the horizontal line indicate whether stimulation was added; + and − below the horizontal line indicate the expression of the indicated marker on the gated CD56^{dim} CD16$^+$ NK cell subpopulation. Each color-filled point represents an individual subject, and horizontal lines represent the group medians. Significance was calculated using a Friedman's test (paired) with a *post hoc* Dunn's test. *P* values were adjusted by multiplying by the number of comparisons made (Bonferroni correction). n.s., no significant difference; **, $P < 0.005$; ***, $P < 0.0005$.

receptors in isolation. High-parameter data sets can be interrogated computationally in an unbiased fashion to uncover novel subsets of cells that may not be identified by more-limited flow cytometry panels.

We identified several clusters that differentiated subjects with or without active HIV viremia, a finding that suggests that NK cell receptor expression may be impacted by the presence of HIV antigens and/or active viral replication. More intriguingly, after LDA dimensionality reduction, the frequencies of cells identified in clusters 7 to 11 correlated with HIV DNA measurements. Importantly, the frequencies of cells identified in cluster 8 and cluster 10 remained significantly correlated with HIV DNA in the analyses that included only aviremic subjects (EC and cART; Fig. 5B). The cells in clusters 7 to 11 were more abundant in EC than in VNC and when combined showed a pattern of receptor expression similar to that seen with cluster 24429 (Fig. 6A).

The NK cell clusters identified from the semisupervised machine learning approaches used in this study are largely distinguished from other CD56^{dim} CD16$^+$ NK cells by their reduced expression of CD57 and increased expression of CD11b, CD161, and Siglec-7.

Some of the markers that define this cell subset have been implicated in previous studies of NK cell function. Siglec-7 is a sialic acid-binding protein that has an immune tyrosine-based inhibition motif (ITIM). Siglec-7 is expressed on highly active NK cells (56), and loss of expression is believed to correspond to dysfunction of NK cells, which occurs in chronic HIV and HCV infection (46, 57). CD11b is a marker of maturation of NK cells in humans and mice (58, 59). CD57 is a marker of terminally matured NK cells (60) and has been suggested to identify antigen-experienced NK cells; consistent with this hypothesis, the frequency of CD57-expressing NK cells is higher in HIV-infected subjects (61). CD161 is a C-type lectin expressed on some T cells and on the majority of NK cells early in maturation (62). CD161 marks cytotoxic NK cells, but interaction with its cognate ligand LLT1 has been shown to repress NK cell function (63, 64). CD161$^+$ NK cells, like CD161$^+$ T cells, have an enhanced ability to respond to cytokines,

including IL-12 and IL-18 (52, 65), and CD161$^+$ CD57$^-$ NK cells have enhanced proliferative capabilities (52). On the basis of the identified marker expression, the CD11b$^+$ CD57$^-$ CD161$^+$ Siglec-7$^+$ CD56^{dim} CD16$^+$ NK cells are likely highly active, partially matured, cytotoxic NK cells (51, 52, 56, 60) and thus might contribute to the spontaneous control of HIV replication in the absence of antiretroviral therapy. Indeed, our *in vitro* data support this hypothesis, as the CD11b$^+$ CD57$^-$ CD161$^+$ Siglec-7$^+$ subpopulation showed a higher response to stimulation than other CD56^{dim} CD16$^+$ NK cell subsets.

NK cells represent a heterogeneous population, and the complexity of NK cell maturation and activation is an area of ongoing investigation. The identification of NK cell clusters that correlate with HIV DNA levels could be a fingerprint of antigen exposure level during the course of infection or, more intriguingly, could reveal NK phenotypes that contribute to the control of viral replication in early stages of infection. The interactions between the identified differentially expressed receptors on antigen-inexperienced CD56^{dim} CD16$^+$ NK cells, including CD11b, CD161, and Siglec-7, and the functional impact of their modulation on the NK cell activity could contribute to better understanding of various distinct mechanisms of HIV control and thus warrant further exploration. Future studies to understand the effect of modulating this NK cell subpopulation would benefit from knowing if a similar subpopulation exists in animal species.

MATERIALS AND METHODS

HIV-infected subject recruitment. Prior to enrollment in the study, all subjects provided informed consent as approved by the Committee on Human Research of the University of California, San Francisco. A total of 93 subjects were recruited from the SCOPE Study cohort as follows: 21 chronically infected, antiretroviral therapy-treated subjects with a viral load of <40 copies/ml of plasma (cART); 12 chronically infected, antiretroviral therapy-naive subjects with a viral load of >5,000 copies/ml of plasma (viremic noncontrollers [VNC]); 27 antiretroviral therapy-naive subjects with a viral load of between 40 and 2,000 copies/ml of plasma (viremic controllers [VC]); 13 antiretroviral therapy-naive subjects with a viral load of <40 copies/ml of plasma (elite controllers [EC]); and 20 HIV-seronegative subjects (HIV-negative [HN]). Viral load measurements were confirmed in-house using the COBAS TaqMan test v2.0. HN were verified as HIV antibody negative by Western blotting. All subjects were screened to have a CD4$^+$ T cell count of >200 cells/μl of blood. All subjects were screened to be HCV antibody negative and/or HCV load negative at the time of donation; HCV antibody positivity was not an exclusion criterion if the subject had undetectable HCV load at the time of sample collection. Additional details are available in Table S1 in the supplemental material.

Sample preparation and storage. Whole blood was collected in acid citrate dextrose (ACD)-containing Vacutainers. Blood was processed on the day of collection. PBMCs were isolated by density centrifugation over Ficoll-Paque media. PBMCs were counted and resuspended at 10 M cells/ml of freezing media (90% fetal bovine serum [FBS], 10% dimethyl sulfoxide [DMSO]). Cells were frozen to −80°C in a controlled-rate freezing chamber. The next morning, samples were transferred to liquid nitrogen storage and maintained at −160°C for long-term storage.

Genomic DNA isolation and cell-associated HIV quantification. Genomic DNA was isolated from thawed PBMCs, and HIV was quantified as previously reported. In brief, genomic DNA was isolated by sonicating cells, treating them with chaotropic salts, and precipitating them with alcohol (41). Genomic DNA isolated from U1 cells (containing 2 copies of integrated HIV/cell) was used to make a standard curve for human genome copy number as well as HIV copy number determinations. CCR5 was used as a standard control for human genome copy number determinations (66). HIV was detected using primers and probes within the HIV integrase gene as previously optimized for the integrase single-copy assay (67). Quantitative PCR (qPCR) was performed using TaqMan Fast Advanced master mix (Thermo Fisher) in a final volume of 25 μl (42).

Mass cytometry Ab validation. Monoclonal antibodies were conjugated to metals isotopes (Table S2) using a MaxPAR antibody conjugation kit (Fluidigm) and were diluted to 0.2 to 0.4 mg/ml in antibody stabilizer phosphate-buffered saline (PBS) (Candor Bioscience). Optimal staining concentrations for each antibody were determined by titrating antibody concentrations prior to staining cell lines and primary cells as positive and negative controls.

Sample processing and data acquisition. Frozen PBMCs were thawed rapidly at 37°C. Prewarmed RPMI 1640 supplemented with 10% FBS and 0.1 mg/ml DNase I was added dropwise in a swirling motion to maximize viability and prevent clumping. Each sample was treated with cisplatin for the exclusion of dead cells (68) and fixed with 1.5% paraformaldehyde. A total of 1×10^6 cells from each sample were aliquoted, and pre-Perm palladium barcoding was performed as previously described (69, 70). Cells were then pooled, treated with Fc receptor blocking solution (BioLegend), and stained with metal-labeled antibodies and DNA intercalators as previously reported (69, 71–73). Cells were washed and resuspended with normalization beads (74) prior to being loaded into a CyTOF 1 instrument for acquisition (Fluidigm).

All samples were run in a total of 6 batches. PBMCs from the same 3 subjects (1 EC, 1 cART, and 1 HN) were included in each run for all 6 batches to verify consistency from run to run.

After acquisition, individual markers were checked to verify that the positive population had been successfully resolved from the negative population. A total of 3 antibodies (2B4, NKp30, and NKp44) showed minimal staining. CD137-positive cells could not be resolved from CD137-negative cells due to high background levels. Those four markers were excluded from downstream analysis. Additionally, t-distributed stochastic neighbor embedding (tSNE) was run to rule out batch effects (data not shown).

Linear regressions and statistical tests. Ordinary least-squares linear regressions were calculated using Python (statsmodels). Pairwise comparisons were performed using a Kruskal-Wallis (KW) test with a *post hoc* Dunn's test (https://gist.github.com/alimuldal/fbb19b73fa25423f02e8) or Friedman's paired test (GraphPad Prism). To correct for false discovery, *P* values corresponding to the KW-Dunn results were further adjusted by multiplying by the number of comparisons made (Bonferroni correction). All reported *P* values were adjusted for multiple testing.

CITRUS analysis. CITRUS (cluster identification, characterization, and regression) (49) was run using a Cytobank platform. $CD56^{bright}$ $CD16^{-}$, $CD56^{dim}$ $CD16^{+}$, and $CD56^{-}$ $CD16^{+}$ $CD7^{+}$ NK cells were downsampled to equal sample sizes for each subject ($CD56^{bright}$ $CD16^{-}$, 206 cells; $CD56^{dim}$ $CD16^{+}$, 1,111 cells; $CD56^{-}$ $CD16^{+}$ $CD7^{+}$, 265 cells). Subjects with too few cells per NK cell subtype were excluded from analysis. Cluster sizes were limited to a minimum of 5% of total cells. HIV-infected subject groups were compared in a pairwise fashion. Cells were concatenated from subjects within the two subject groups being compared. After unsupervised agglomerative hierarchical clustering, cluster abundances were inputted into a LASSO-regularized logistic regression to build a logistic classifier; hyperparameters were optimized using k-fold cross-validation.

Dimensionality reduction and cluster identification. The downsampled data used for CITRUS were used also for principal-component analysis (PCA), linear discriminant analysis (LDA), and tSNE using Python (scikit-learn). PCA prioritizes describing data sets as a combination of attributes (e.g., in this study, individual marker intensities), representing their variation through principal components (PCs), which preserve as much variance in the data set as possible. The focus of tSNE is to deconvolute high-parameter data by identifying similarities between data points (e.g., in this study, individual cells) and then projecting the relationships in two dimensions. Both of these approaches preserve the information in a data set in an attempt to portray the data in a way that allows the user to identify new clusters in an agnostic fashion (e.g., in this study, to identify NK cell subpopulations without taking HIV-infected subject groups into consideration). LDA is a supervised dimensionality reduction algorithm that identifies combinations of attributes (e.g., in this study, individual marker intensities) that maximize the separation of a given response variable (e.g., in this study, HIV subject groups); LDA does not maintain the overall variance of the data set but separates the data points based on response variables more effectively (e.g., in this study, identified the NK cell subpopulations that differentiated HIV-infected subject groups). tSNE was run with a random seed, a maximum of 5,000 iterations, and perplexity set to 50, using the Barnes-Hut approximation (angle = 0.5). LDA was run using eigenvalue decomposition and was limited to two dimensions. Clusters were subsequently identified by k-means clustering using the ACCENSE package (50).

NK cell functional assays. Frozen PBMCs were thawed rapidly at 37°C and washed in RPMI 1640 supplemented with 10% FBS. Cells were rested at 37°C and 5% CO_2 for 3 h prior to enrichment of NK cells (Stemcell Technologies). After being rested overnight at 37°C and 5% CO_2, 2×10^5 NK cells were plated in individual wells of a 96-well flat bottom plate and stimulated with either cytokines (10 ng/ml IL-12 [BioLegend] plus 100 ng/ml IL-18 [BioLegend]) or K562 cells (10:1 effector/target ratio) for 5 h at 37°C and 5% CO_2. After the first hour of stimulation, brefeldin A (BioLegend), monensin (BioLegend), and CD107a (clone H4A3; BioLegend) were added. After stimulation, cells were stained for viability (Zombie dyes; BioLegend), CD3 (clone UCHT1; BioLegend), CD11b (clone ICRF44; BioLegend), CD16 (clone 3G8; BioLegend), CD56 (clone HDC56; BioLegend), CD57 (clone H CD57; BioLegend), CD161 (clone 191B8; Miltenyi Biotec), and Siglec-7 (clone 6 to 434; BioLegend). Cells were fixed and permeabilized with CytoFix/CytoPerm reagent (BD Biosciences) prior to staining for intracellular IFN-γ (clone B27; BioLegend). Stained cells were analyzed on an LSRFortessa X-20 instrument (BD Biosciences), and data were analyzed using FlowJo (TreeStar).

SUPPLEMENTAL MATERIAL

Supplemental material for this article may be found at https://doi.org/10.1128/JVI.01790-18.

SUPPLEMENTAL FILE 1, PDF file, 1 MB.

ACKNOWLEDGMENTS

All of us who are affiliated with Gilead Sciences own shares in the company. Additionally, S.G.D. receives research support from Gilead, Merck, and ViiV; has consulted for AbbVie and Janssen; and is an advisor for Enochian Biosciences and Bryologix. G.P.N. is a paid consultant for Fluidigm, the manufacturer that produced some of the reagents and instrumentation used in this study.

REFERENCES

1. Siliciano JD, Kajdas J, Finzi D, Quinn TC, Chadwick K, Margolick JB, Kovacs C, Gange SJ, Siliciano RF. 2003. Long-term follow-up studies confirm the stability of the latent reservoir for HIV-1 in resting CD4+ T cells. Nat Med 9:727–728. https://doi.org/10.1038/nm880.
2. Crooks AM, Bateson R, Cope AB, Dahl NP, Griggs MK, Kuruc JD, Gay CL, Eron JJ, Margolis DM, Bosch RJ, Archin NM. 2015. Precise quantitation of the latent HIV-1 reservoir: implications for eradication strategies. J Infect Dis 212:1361–1365. https://doi.org/10.1093/infdis/jiv218.
3. Lifson AR, Buchbinder SP, Sheppard HW, Mawle AC, Wilber JC, Stanley M, Hart CE, Hessol NA, Holmberg SD. 1991. Long-term human immunodeficiency virus infection in asymptomatic homosexual and bisexual men with normal CD4+ lymphocyte counts: immunologic and virologic characteristics. J Infect Dis 163:959–965. https://doi.org/10.1093/infdis/163.5.959.
4. Lambotte O, Boufassa F, Madec Y, Nguyen A, Goujard C, Meyer L, Rouzioux C, Venet A, Delfraissy JF. 2005. HIV controllers: a homogeneous group of HIV-1-infected patients with spontaneous control of viral replication. Clin Infect Dis 41:1053–1056. https://doi.org/10.1086/433188.
5. Madec Y, Boufassa F, Porter K, Meyer L. 2005. Spontaneous control of viral load and CD4 cell count progression among HIV-1 seroconverters. AIDS 19:2001–2007. https://doi.org/10.1097/01.aids.0000194134.28135.cd.
6. Deeks SG, Walker BD. 2007. Human immunodeficiency virus controllers: mechanisms of durable virus control in the absence of antiretroviral therapy. Immunity 27:406–416. https://doi.org/10.1016/j.immuni.2007.08.010.
7. Mikulak J, Oriolo F, Zaghi E, Di Vito C, Mavilio D. 2017. Natural killer cells in HIV-1 infection and therapy. AIDS 31:2317–2330. https://doi.org/10.1097/QAD.0000000000001645.
8. Migueles SA, Sabbaghian MS, Shupert WL, Bettinotti MP, Marincola FM, Martino L, Hallahan CW, Selig SM, Schwartz D, Sullivan J, Connors M. 2000. HLA B*5701 is highly associated with restriction of virus replication in a subgroup of HIV-infected long term nonprogressors. Proc Natl Acad Sci U S A 97:2709–2714. https://doi.org/10.1073/pnas.050567397.
9. Pereyra F, Jia X, McLaren PJ, Telenti A, de Bakker PIW, Walker BD, Ripke S, Brumme CJ, Pulit SL, Carrington M, Kadie CM, Carlson JM, Heckerman D, Graham RR, Plenge RM, Deeks SG, Gianniny L, Crawford G, Sullivan J, Gonzalez E, Davies L, Camargo A, Moore JM, Beattie N, Gupta S, Crenshaw A, Burtt NP, Guiducci C, Gupta N, Gao X, Qi Y, Yuki Y, Piechocka-Trocha A, Cutrell E, Rosenberg R, Moss KL, Lemay P, O'Leary J, Schaefer T, Verma P, Toth I, Block B, Baker B, Rothchild A, Lian J, Proudfoot J, Alvino DML, Vine S, Addo MM, Allen TM, et al. 2010. The major genetic determinants of HIV-1 control affect HLA class I peptide presentation. Science 330:1551–1557. https://doi.org/10.1126/science.1195271.
10. Migueles SA, Laborico AC, Shupert WL, Sabbaghian MS, Rabin R, Hallahan CW, Van Baarle D, Kostense S, Miedema F, McLaughlin M, Ehler L, Metcalf J, Liu S, Connors M. 2002. HIV-specific CD8+ T cell proliferation is coupled to perforin expression and is maintained in nonprogressors. Nat Immunol 3:1061–1068. https://doi.org/10.1038/ni845.
11. Betts MR, Nason MC, West SM, De Rosa SC, Migueles SA, Abraham J, Lederman MM, Benito JM, Goepfert PA, Connors M, Roederer M, Koup RA. 2006. HIV nonprogressors preferentially maintain highly functional HIV-specific CD8+ T cells. Blood 107:4781–4789. https://doi.org/10.1182/blood-2005-12-4818.
12. Saez-Cirion A, Lacabaratz C, Lambotte O, Versmisse P, Urrutia A, Boufassa F, Barre-Sinoussi F, Delfraissy JF, Sinet M, Pancino G, Venet A. 2007. HIV controllers exhibit potent CD8 T cell capacity to suppress HIV infection ex vivo and peculiar cytotoxic T lymphocyte activation phenotype. Proc Natl Acad Sci U S A 104:6776–6781. https://doi.org/10.1073/pnas.0611244104.
13. Almeida JR, Price DA, Papagno L, Arkoub ZA, Sauce D, Bornstein E, Asher TE, Samri A, Schnuriger A, Theodorou I, Costagliola D, Rouzioux C, Agut H, Marcelin AG, Douek D, Autran B, Appay V. 2007. Superior control of HIV-1 replication by CD8+ T cells is reflected by their avidity, polyfunctionality, and clonal turnover. J Exp Med 204:2473–2485. https://doi.org/10.1084/jem.20070784.
14. Ferre AL, Hunt PW, Critchfield JW, Young DH, Morris MM, Garcia JC, Pollard RB, Yee HF, Jr, Martin JN, Deeks SG, Shacklett BL. 2009. Mucosal immune responses to HIV-1 in elite controllers: a potential correlate of immune control. Blood 113:3978–3989. https://doi.org/10.1182/blood-2008-10-182709.
15. Buckheit RW, Salgado M, Silciano RF, Blankson JN. 2012. Inhibitory potential of subpopulations of CD8+ T cells in HIV-1-infected elite suppressors. J Virol 86:13679–13688. https://doi.org/10.1128/JVI.02439-12.
16. Emu B, Sinclair E, Hatano H, Ferre A, Shacklett B, Martin JN, McCune JM, Deeks SG. 2008. HLA class I-restricted T-cell responses may contribute to the control of human immunodeficiency virus infection, but such responses are not always necessary for long-term virus control. J Virol 82:5398–5407. https://doi.org/10.1128/JVI.02176-07.
17. O'Connell KA, Han Y, Williams TM, Siliciano RF, Blankson JN. 2009. Role of natural killer cells in a cohort of elite suppressors: low frequency of the protective KIR3DS1 allele and limited inhibition of human immunodeficiency virus type 1 replication in vitro. J Virol 83:5028–5034. https://doi.org/10.1128/JVI.02551-08.
18. Martin MP, Gao X, Lee JH, Nelson GW, Detels R, Goedert JJ, Buchbinder S, Hoots K, Vlahov D, Trowsdale J, Wilson M, O'Brien SJ, Carrington M. 2002. Epistatic interaction between KIR3DS1 and HLA-B delays the progression to AIDS. Nat Genet 31:429–434. https://doi.org/10.1038/ng934.
19. Martin MP, Qi Y, Gao X, Yamada E, Martin JN, Pereyra F, Colombo S, Brown EE, Shupert WL, Phair J, Goedert JJ, Buchbinder S, Kirk GD, Telenti A, Connors M, O'Brien SJ, Walker BD, Parham P, Deeks SG, McVicar DW, Carrington M. 2007. Innate partnership of HLA-B and KIR3DL1 subtypes against HIV-1. Nat Genet 39:733–740. https://doi.org/10.1038/ng2035.
20. Alter G, Martin MP, Teigen N, Carr WH, Suscovich TJ, Schneidewind A, Streeck H, Waring M, Meier A, Brander C, Lifson JD, Allen TM, Carrington M, Altfeld M. 2007. Differential natural killer cell-mediated inhibition of HIV-1 replication based on distinct KIR/HLA subtypes. J Exp Med 204:3027–3036. https://doi.org/10.1084/jem.20070695.
21. Walker-Sperling VE, Pohlmeyer CW, Veenhuis RT, May M, Luna KA, Kirkpatrick AR, Laeyendecker O, Cox AL, Carrington M, Bailey JR, Arduino RC, Blankson JN. 2017. Factors associated with the control of viral replication and virologic breakthrough in a recently infected HIV-1 controller. EBioMedicine 16:141–149. https://doi.org/10.1016/j.ebiom.2017.01.034.
22. Cooper MA, Fehniger TA, Caligiuri MA. 2001. The biology of human natural killer-cell subsets. Trends Immunol 22:633–640. https://doi.org/10.1016/S1471-4906(01)02060-9.
23. Hu PF, Hultin LE, Hultin P, Hausner MA, Hirji K, Jewett A, Bonavida B, Detels R, Giorgi JV. 1995. Natural killer cell immunodeficiency in HIV disease is manifest by profoundly decreased numbers of CD16+ CD56+ cells and expansion of a population of CD16dim CD56- cells with low lytic activity. J Acquir Immune Defic Syndr Hum Retrovirol 10:331–340.
24. Mavilio D, Benjamin J, Daucher M, Lombardo G, Kottilil S, Planta MA, Marcenaro E, Bottino C, Moretta L, Moretta A, Fauci AS. 2003. Natural killer cells in HIV-1 infection: dichotomous effects of viremia on inhibitory and activating receptors and their functional correlates. Proc Natl Acad Sci U S A 100:15011–15016. https://doi.org/10.1073/pnas.2336091100.
25. Alter G, Teigen N, Davis BT, Addo MM, Suscovich TJ, Waring MT, Streeck H, Johnston MN, Staller KD, Zaman MT, Yu XG, Lichterfeld M, Basgoz N, Rosenberg ES, Altfeld M. 2005. Sequential deregulation of NK cell subset distribution and function starting in acute HIV-1 infection. Blood 106:3366–3369. https://doi.org/10.1182/blood-2005-03-1100.
26. Milush JM, López-Vergès S, York VA, Deeks SG, Martin JN, Hecht FM, Lanier LL, Nixon DF. 2013. CD56neg CD16(+) NK cells are activated mature NK cells with impaired effector function during HIV-1 infection. Retrovirology 10:158. https://doi.org/10.1186/1742-4690-10-158.
27. Bjorkstrom NK, Ljunggren HG, Sandberg JK. 2010. CD56 negative NK cells: origin, function, and role in chronic viral disease. Trends Immunol 31:401–406. https://doi.org/10.1016/j.it.2010.08.003.
28. Gonzalez VD, Falconer K, Michaelsson J, Moll M, Reichard O, Alaeus A, Sandberg JK. 2008. Expansion of CD56- NK cells in chronic HCV/HIV-1 co-infection: reversion by antiviral treatment with pegylated IFNalpha and ribavirin. Cl Immunol 128:46–56. https://doi.org/10.1016/j.clim.2008.03.521.
29. Gonzalez VD, Falconer K, Bjorkstrom NK, Blom KG, Weiland O, Ljunggren HG, Alaeus A, Sandberg JK. 2009. Expansion of functionally skewed CD56-negative NK cells in chronic hepatitis C virus infection: correlation with outcome of pegylated IFN-alpha and ribavirin treatment. J Immunol 183:6612–6618. https://doi.org/10.4049/jimmunol.0901437.
30. Lanier LL. 1998. NK cell receptors. Annu Rev Immunol 16:359–393. https://doi.org/10.1146/annurev.immunol.16.1.359.
31. Boulet S, Kleyman M, Kim JY, Kamya P, Sharafi S, Simic N, Bruneau J, Routy JP, Tsoukas CM, Bernard NF. 2008. A combined genotype of

KIR3DL1 high expressing alleles and HLA-B*57 is associated with a reduced risk of HIV infection. AIDS 22:1487–1491. https://doi.org/10.1097/QAD.0b013e3282ffde7e.
32. Boulet S, Sharafi S, Simic N, Bruneau J, Routy JP, Tsoukas CM, Bernard NF. 2008. Increased proportion of KIR3DS1 homozygotes in HIV-exposed uninfected individuals. AIDS 22:595–599. https://doi.org/10.1097/QAD.0b013e3282f56b23.
33. Alter G, Heckerman D, Schneidewind A, Fadda L, Kadie CM, Carlson JM, Oniangue-Ndza C, Martin M, Li B, Khakoo SI, Carrington M, Allen TM, Altfeld M. 2011. HIV-1 adaptation to NK-cell-mediated immune pressure. Nature 476:96–100. https://doi.org/10.1038/nature10237.
34. Ramsuran V, Naranbhai V, Horowitz A, Qi Y, Martin MP, Yuki Y, Gao X, Walker-Sperling V, Del Prete GQ, Schneider DK, Lifson JD, Fellay J, Deeks SG, Martin JN, Goedert JJ, Wolinsky SM, Michael NL, Kirk GD, Buchbinder S, Haas D, Ndung'u T, Goulder P, Parham P, Walker BD, Carlson JM, Carrington M. 2018. Elevated HLA-A expression impairs HIV control through inhibition of NKG2A-expressing cells. Science 359:86–90. https://doi.org/10.1126/science.aam8825.
35. Tomescu C, Mavilio D, Montaner LJ. 2015. Lysis of HIV-1-infected autologous CD4+ primary T cells by interferon-alpha-activated NK cells requires NKp46 and NKG2D. AIDS 29:1767–1773. https://doi.org/10.1097/QAD.0000000000000777.
36. Cerboni C, Neri F, Casartelli N, Zingoni A, Cosman D, Rossi P, Santoni A, Doria M. 2007. Human immunodeficiency virus 1 Nef protein downmodulates the ligands of the activating receptor NKG2D and inhibits natural killer cell-mediated cytotoxicity. J Gen Virol 88:242–250. https://doi.org/10.1099/vir.0.82125-0.
37. Schwartz O, Marechal V, Le Gall S, Lemonnier F, Heard JM. 1996. Endocytosis of major histocompatibility complex class I molecules is induced by the HIV-1 Nef protein. Nat Med 2:338–342. https://doi.org/10.1038/nm0396-338.
38. De Maria A, Fogli M, Costa P, Murdaca G, Puppo F, Mavilio D, Moretta A, Moretta L. 2003. The impaired NK cell cytolytic function in viremic HIV-1 infection is associated with a reduced surface expression of natural cytotoxicity receptors (NKp46, NKp30 and NKp44). Eur J Immunol 33:2410–2418. https://doi.org/10.1002/eji.200324141.
39. Vieillard V, Fausther-Bovendo H, Samri A, Debré P. 2010. Specific phenotypic and functional features of natural killer cells from HIV-infected long-term nonprogressors and HIV controllers. J Acquir Immune Defic Syndr 53:564–573. https://doi.org/10.1097/QAI.0b013e3181d0c5b4.
40. Marras F, Casabianca A, Bozzano F, Ascierto ML, Orlandi C, Di Biagio A, Pontali E, Dentone C, Orofino G, Nicolini L, Taramasso L, Magnani M, Marincola FM, Wang E, Moretta L, De Maria A. 2017. Control of the HIV-1 DNA reservoir is associated in vivo and in vitro with NKp46/NKp30 (CD335 CD337) inducibility and interferon gamma production by transcriptionally unique NK cells. J Virol 91:e00647-17. https://doi.org/10.1128/JVI.00647-17.
41. Hong F, Aga E, Cillo AR, Yates AL, Besson G, Fyne E, Koontz DL, Jennings C, Zheng L, Mellors JW. 2016. Novel assays for measurement of total cell-associated HIV-1 DNA and RNA. J Clin Microbiol 54:902–911. https://doi.org/10.1128/JCM.02904-15.
42. Sloan DD, Lam CY, Irrinki A, Liu L, Tsai A, Pace CS, Kaur J, Murry JP, Balakrishnan M, Moore PA, Johnson S, Nordstrom JL, Cihlar T, Koenig S. 2015. Targeting HIV reservoir in infected CD4 T cells by dual-affinity re-targeting molecules (DARTs) that bind HIV envelope and recruit cytotoxic T cells. PLoS Pathog 11:e1005233. https://doi.org/10.1371/journal.ppat.1005233.
43. Eriksson S, Graf EH, Dahl V, Strain MC, Yukl SA, Lysenko ES, Bosch RJ, Lai J, Chioma S, Emad F, Abdel-Mohsen M, Hoh R, Hecht F, Hunt P, Somsouk M, Wong J, Johnston R, Siliciano RF, Richman DD, O'Doherty U, Palmer S, Deeks SG, Siliciano JD. 2013. Comparative analysis of measures of viral reservoirs in HIV-1 eradication studies. PLoS Pathog 9:e1003174. https://doi.org/10.1371/journal.ppat.1003174.
44. Rouzioux C, Richman D. 2013. How to best measure HIV reservoirs? Curr Opin HIV AIDS 8:170–175. https://doi.org/10.1097/COH.0b013e32835fc619.
45. Marras F, Nicco E, Bozzano F, Di Biagio A, Dentone C, Pontali E, Boni S, Setti M, Orofino G, Mantia E, Bartolacci V, Bisio F, Riva A, Biassoni R, Moretta L, De Maria A. 2013. Natural killer cells in HIV controller patients express an activated effector phenotype and do not up-regulate NKp44 on IL-2 stimulation. Proc Natl Acad Sci U S A 110:11970–11975. https://doi.org/10.1073/pnas.1302090110.
46. Brunetta E, Fogli M, Varchetta S, Bozzo L, Hudspeth KL, Marcenaro E, Moretta A, Mavilio D. 2009. The decreased expression of Siglec-7 represents an early marker of dysfunctional natural killer-cell subsets associated with high levels of HIV-1 viremia. Blood 114:3822–3830. https://doi.org/10.1182/blood-2009-06-226332.
47. Titanji K, Sammicheli S, De Milito A, Mantegani P, Fortis C, Berg L, Kärre K, Travi G, Tassandin C, Lopalco L, Rethi B, Tambussi G, Chiodi F. 2008. Altered distribution of natural killer cell subsets identified by CD56, CD27 and CD70 in primary and chronic human immunodeficiency virus-1 infection. Immunology 123:164–170. https://doi.org/10.1111/j.1365-2567.2007.02657.x.
48. Zulu MZ, Naidoo KK, Mncube Z, Jaggernath M, Goulder PJR, Ndung'u T, Altfeld M, Thobakgale CF. 2017. Reduced expression of Siglec-7, NKG2A, and CD57 on terminally differentiated CD56(-) CD16(+) natural killer cell subset is associated with natural killer cell dysfunction in chronic HIV-1 clade C infection. AIDS Res Hum Retroviruses 33:1205–1213. https://doi.org/10.1089/AID.2017.0095.
49. Bruggner RV, Bodenmiller B, Dill DL, Tibshirani RJ, Nolan GP. 2014. Automated identification of stratifying signatures in cellular subpopulations. Proc Natl Acad Sci U S A 111:E2770–E2777. https://doi.org/10.1073/pnas.1408792111.
50. Shekhar K, Brodin P, Davis MM, Chakraborty AK. 2014. Automatic classification of cellular expression by nonlinear stochastic embedding (ACCENSE). Proc Natl Acad Sci U S A 111:202–207. https://doi.org/10.1073/pnas.1321405111.
51. Fu B, Wang F, Sun R, Ling B, Tian Z, Wei H. 2011. CD11b and CD27 reflect distinct population and functional specialization in human natural killer cells. Immunology 133:350–359. https://doi.org/10.1111/j.1365-2567.2011.03446.x.
52. Kurioka A, Cosgrove C, Simoni Y, van Wilgenburg B, Geremia A, Björkander S, Sverremark-Ekström E, Thurnheer C, Günthard HF, Khanna N, Walker LJ, Arancibia-Cárcamo CV, Newell EW, Willberg CB, Klenerman P. 2018. CD161 defines a functionally distinct subset of pro-inflammatory natural killer cells. Front Immunol 9:486. https://doi.org/10.3389/fimmu.2018.00486.
53. Martinet L, Ferrari De Andrade L, Guillerey C, Lee JS, Liu J, Souza-Fonseca-Guimaraes F, Hutchinson DS, Kolesnik TB, Nicholson SE, Huntington ND, Smyth MJ. 2015. DNAM-1 expression marks an alternative program of NK cell maturation. Cell Rep 11:85–97. https://doi.org/10.1016/j.celrep.2015.03.006.
54. Kruse PH, Matta J, Ugolini S, Vivier E. 2014. Natural cytotoxicity receptors and their ligands. Immunol Cell Biol 92:221–229. https://doi.org/10.1038/icb.2013.98.
55. Lopez-Vergès S, Milush JM, Pandey S, York VA, Arakawa-Hoyt J, Pircher H, Norris PJ, Nixon DF, Lanier LL. 2010. CD57 defines a functionally distinct population of mature NK cells in the human CD56dim CD16+ NK-cell subset. Blood 116:3865–3874. https://doi.org/10.1182/blood-2010-04-282301.
56. Shao JY, Yin WW, Zhang QF, Liu Q, Peng ML, Hu HD, Hu P, Ren H, Zhang DZ. 2016. Siglec-7 defines a highly functional natural killer cell subset and inhibits cell-mediated activities. Scand J Immunol 84:182–190. https://doi.org/10.1111/sji.12455.
57. Varchetta S, Mele D, Lombardi A, Oliviero B, Mantovani S, Tinelli C, Spreafico M, Prati D, Ludovisi S, Ferraioli G, Filice C, Aghemo A, Lampertico P, Facchetti F, Bernuzzi F, Invernizzi P, Mondelli MU. 2016. Lack of Siglec-7 expression identifies a dysfunctional natural killer cell subset associated with liver inflammation and fibrosis in chronic HCV infection. Gut 65:1998–2006. https://doi.org/10.1136/gutjnl-2015-310327.
58. Hayakawa Y, Huntington ND, Nutt SL, Smyth MJ. 2006. Functional subsets of mouse natural killer cells. Immunol Rev 214:47–55. https://doi.org/10.1111/j.1600-065X.2006.00454.x.
59. Fu B, Tian Z, Wei H. 2014. Subsets of human natural killer cells and their regulatory effects. Immunology 141:483–489. https://doi.org/10.1111/imm.12224.
60. Nielsen CM, White MJ, Goodier MR, Riley EM. 2013. Functional significance of CD57 expression on human NK cells and relevance to disease. Front Immunol 4:422. https://doi.org/10.3389/fimmu.2013.00422.
61. Hong HS, Eberhard JM, Keudel P, Bollmann BA, Ballmaier M, Bhatnagar N, Zielinska-Skowronek M, Schmidt RE, Meyer-Olson D. 2010. HIV infection is associated with a preferential decline in less-differentiated CD56dim CD16+ NK cells. J Virol 84:1183–1188. https://doi.org/10.1128/JVI.01675-09.
62. Bennett IM, Zatsepina O, Zamai L, Azzoni L, Mikheeva T, Perussia B. 1996. Definition of a natural killer NKR-P1A+/CD56-/CD16$^-$ functionally immature human NK cell subset that differentiates in vitro in the presence of interleukin 12. J Exp Med 184:1845–1856. https://doi.org/10.1084/jem.184.5.1845.

63. Aldemir H, Prod'homme V, Dumaurier MJ, Retiere C, Poupon G, Cazareth J, Bihl F, Braud VM. 2005. Cutting edge: lectin-like transcript 1 is a ligand for the CD161 receptor. J Immunol 175:7791–7795. https://doi.org/10.4049/jimmunol.175.12.7791.
64. Rosen DB, Bettadapura J, Alsharifi M, Mathew PA, Warren HS, Lanier LL. 2005. Cutting edge: lectin-like transcript-1 is a ligand for the inhibitory human NKR-P1A receptor. J Immunol 175:7796–7799. https://doi.org/10.4049/jimmunol.175.12.7796.
65. Orange JS, Wang B, Terhorst C, Biron CA. 1995. Requirement for natural killer cell-produced interferon gamma in defense against murine cytomegalovirus infection and enhancement of this defense pathway by interleukin 12 administration. J Exp Med 182:1045–1056. https://doi.org/10.1084/jem.182.4.1045.
66. Malnati MS, Scarlatti G, Gatto F, Salvatori F, Cassina G, Rutigliano T, Volpi R, Lusso P. 2008. A universal real-time PCR assay for the quantification of group-M HIV-1 proviral load. Nat Protoc 3:1240–1248. https://doi.org/10.1038/nprot.2008.108.
67. Cillo AR, Krishnan A, Mitsuyasu RT, McMahon DK, Li S, Rossi JJ, Zaia JA, Mellors JW. 2013. Plasma viremia and cellular HIV-1 DNA persist despite autologous hematopoietic stem cell transplantation for HIV-related lymphoma. J Acquir Immune Defic Syndr 63:438–441. https://doi.org/10.1097/QAI.0b013e31828e6163.
68. Fienberg HG, Simonds EF, Fantl WJ, Nolan GP, Bodenmiller B. 2012. A platinum-based covalent viability reagent for single-cell mass cytometry. Cytometry A 81:467–475. https://doi.org/10.1002/cyto.a.22067.
69. Behbehani GK, Thom C, Zunder ER, Finck R, Gaudilliere B, Fragiadakis GK, Fantl WJ, Nolan GP. 2014. Transient partial permeabilization with saponin enables cellular barcoding prior to surface marker staining. Cytometry A 85:1011–1019. https://doi.org/10.1002/cyto.a.22573.
70. Zunder ER, Finck R, Behbehani GK, Amir ED, Krishnaswamy S, Gonzalez VD, Lorang CG, Bjornson Z, Spitzer MH, Bodenmiller B, Fantl WJ, Pe'er D, Nolan GP. 2015. Palladium-based mass tag cell barcoding with a doublet-filtering scheme and single-cell deconvolution algorithm. Nat Protoc 10:316–333. https://doi.org/10.1038/nprot.2015.020.
71. Bendall SC, Simonds EF, Qiu P, Amir ED, Krutzik PO, Finck R, Bruggner RV, Melamed R, Trejo A, Ornatsky OI, Balderas RS, Plevritis SK, Sachs K, Pe'er D, Tanner SD, Nolan GP. 2011. Single-cell mass cytometry of differential immune and drug responses across a human hematopoietic continuum. Science 332:687–696. https://doi.org/10.1126/science.1198704.
72. Gaudillière B, Fragiadakis GK, Bruggner RV, Nicolau M, Finck R, Tingle M, Silva J, Ganio EA, Yeh CG, Maloney WJ, Huddleston JI, Goodman SB, Davis MM, Bendall SC, Fantl WJ, Angst MS, Nolan GP. 2014. Clinical recovery from surgery correlates with single-cell immune signatures. Sci Transl Med 6:255ra131. https://doi.org/10.1126/scitranslmed.3009701.
73. Gonzalez VD, Samusik N, Chen TJ, Savig ES, Aghaeepour N, Quigley DA, Huang YW, Giangarrà V, Borowsky AD, Hubbard NE, Chen SY, Han G, Ashworth A, Kipps TJ, Berek JS, Nolan GP, Fantl WJ. 2018. Commonly occurring cell subsets in high-grade serous ovarian tumors identified by single-cell mass cytometry. Cell Rep 22:1875–1888. https://doi.org/10.1016/j.celrep.2018.01.053.
74. Finck R, Simonds EF, Jager A, Krishnaswamy S, Sachs K, Fantl W, Pe'er D, Nolan GP, Bendall SC. 2013. Normalization of mass cytometry data with bead standards. Cytometry A 83:483–494. https://doi.org/10.1002/cyto.a.22271.